

# FRETTING FATIGUE AND THEORY OF CRITICAL DISTANCE: LINE AND POINT METHODS APPLIED ON PREDICTION OF FATIGUE STRENGTH FOR CYLINDRICAL CONTACTS UNDER A PARTIAL SLIP REGIME

**Luiz Homero Lopes Martins, luiz\_unb@hotmail.com**

University of Brasília, Department of Mechanical Engineering, Brasília-DF-Brazil, CEP 70910-900

**José Alexander Araújo, alex07@unb.br**

University of Brasília, Department of Mechanical Engineering, Brasília-DF-Brazil, CEP 70910-900

**Júlio César Torres Ferro, Jct.ferro@gmail.com**

University of Brasília, Department of Mechanical Engineering, Brasília-DF-Brazil, CEP 70910-900

**Abstract.** *The aim of this work is to propose a methodology to estimate the fatigue strength limit under fretting conditions which was validated for experimental results taken from the literature for contact between cylindrical pads. This methodology is founded on the use of the Theory of Critical Distance (LineMethod) associated with the multiaxial fatigue model proposed by Susmel & Lazzarin (Modified Wöhler Curve Method). The results provided by the Line Method and the Point Method were compared showing that the Line Method was less conservative than the Point Method. The Line Method has correctly evaluated, rightly, the fatigue strength for 26 of 29 experimental tests, against 23 of 29 for the Point Method. Both methods were also compared concerning their sensibility to an increase or decrease of 10% on the value of the material parameter that determine the critical distance which was used to apply the multiaxial fatigue model. The results have shown that the Line Method is less sensitive than the Point Method to this parameter for high stress gradients.*

**Keywords:** *fretting fatigue, notch fatigue, multiaxial fatigue, critical distance, size effect, point method, line method.*

## 1. INTRODUCTION

Some recent findings (Araújo et al., 2004, Vallellano et al., 2004) show that the problem of estimating fatigue endurance under fretting conditions can be addressed by taking into account the presence of stress concentration phenomena. To be precise, the material cracking behaviour under fretting fatigue can be assumed to be similar to that occurring in "conventional" notched components under fatigue loading: crack initiation, and its initial growth, depends on the distribution of the entire stress field damaging the fatigue process zone. This analogy is very attractive from a scientific point of view, because it would allow engineers engaged in practical problems to extend the theories already developed to assess notched components under fatigue loading to components damaged by fretting fatigue. The main problem in coherently extending this idea to practical situations is that the early stage of crack propagation under fretting fatigue is mixed mode dominated (Araújo and Nowell, 1999).

In particular, according to the experimental results published by Vallellano et al. (Vallellano et al., 2004) and generated by testing Al 7075-T6 sphere-plane contacts, initiation and early growth of cracks occur at small angles to the surface. Subsequently, cracks change their direction to grow along a line almost perpendicular to the contact zone surface. Finally, the above authors highlighted that even when failures did not occur in the high-cycle fatigue regime, cracks were arrested by the first grain boundary (as it happens to plain metal specimens under conventional fatigue loading). This experimental finding makes it evident that, to correctly model the physical processes leading to crack initiation and its initial propagation under fretting fatigue, two fundamental aspects should be taken into account: the real material morphology in the vicinity of crack initiation sites and the elasto-plastic behaviour of grains. In other words, predicting the material strength in the high-cycle fretting fatigue regime is mainly a short crack problem. Unfortunately, it is well-known that to correctly model short crack behaviour, linear-elastic approaches may not be the most adequate ones. It is evident that modelling all the phenomena taking place within the fatigue process zone by accounting for grain plasticity is very attractive from a philosophical point of view, but such an approach would be too cumbersome to be applied to assess real components in situations of practical interest. For this reason, the problem must be greatly simplified in order to develop approaches which can be used in the industrial reality.

According to the considerations reported above, this paper attempts to estimate fretting fatigue damage by using a multiaxial fatigue method we recently developed to assess notched components in the high-cycle fatigue regime (Susmel and Taylor, 2003): the aim of this work is to predict fretting fatigue damage accounting for the entire stress field in the vicinity of the contact zone by considering a notch analogue.

## 2. FATIGUE DAMAGE AND STRUCTURAL VOLUME

The use of the Modified Wöhler Curve Method (MWCMM) in conjunction with the Theory of Critical Distances (TCD) is based on the assumption that all the physical processes leading to crack initiation are confined within the so-called structural volume. The size of this volume is assumed not to be dependent on either the stress concentration feature weakening the component or the complexity of the stress field damaging the fatigue process zone (Susmel, 2004).

To define the size of this volume, consider an infinite plate with a central through-crack (Fig. 1a). This plate is subjected to a remote fully-reversed uniaxial fatigue loading ( $R=-1$ ). Observing that, thanks to the above assumptions, geometry, nominal stress gradient and non-zero mean stress do not affect the crack growth, the above configuration can be assumed to be representative of the "pure" material cracking behaviour.

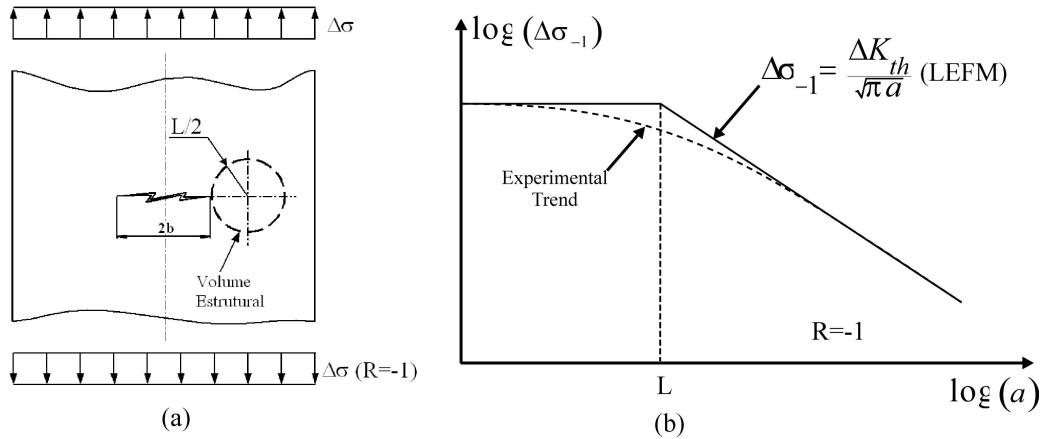


Figure 1. Central through-crack in an infinite plate subjected to a remote uniaxial load (a) and Kitagawa and Takahashi's diagram (b).

Consider now the classical Kitagawa-Takahashi curve by approximating it to the two straight asymptotic lines plotted in Fig. 1b: the horizontal line corresponds to the plain fatigue limit, whereas the sloping one is plotted according to the Linear Elastic Fracture Mechanics (LEFM). The length at which these two lines intersect each other turns out to be:

$$L = \frac{1}{\pi} \left( \frac{\Delta K_{th}}{\Delta \sigma_{-1}} \right)^2 \quad (1)$$

In the above equation,  $\Delta \sigma_{-1}$  is the plain fatigue limit and  $\Delta K_{th}$  is the range of the threshold value of the stress intensity factor (both determined under load ratios,  $R$ , equal to -1). Based on the fact that the material characteristic length  $L$  is defined by two material properties, it is evident that  $L$  turns out to be a material property, which is different for different materials (Taylor, 1999). Observing now the trend schematised by the two straight asymptotic lines in Kitagawa-Takahashi's diagram, it is possible to assume that as long as the half-length of the crack is lower than  $L$ , no reduction of the nominal fatigue limit occurs. Therefore, the size of the structural volume can be considered to be directly related to the material characteristic length,  $L$ . To be precise, in order to avoid a reduction of the nominal fatigue limit, all the cracking processes must be confined within this area, which can be supposed to be circular in 2D bodies and spherical in 3D components (Fig. 1a).

It is possible to observe now that when a component is in the fatigue limit condition some micro/meso-cracks are always present within the structural volume, and it holds true independently of the stress concentration feature weakening the component (Akiniwa et al., 2001). In particular, it is important to remember that the sharper the notches are then the longer the length of non-propagating cracks. When plain specimens are in the fatigue limit condition, the crack propagation is arrested either by the first grain boundary or by the first micro-structural barrier (Miller, 1993). On the contrary, in the presence of sharp notches, the maximum length of non-propagating cracks is equal to:

$$b_0 = \frac{1}{\pi} \left( \frac{\Delta K_{th}}{F \Delta \sigma_{-1}} \right)^2 \quad (2)$$

where  $F$  is the geometrical correction factor for the LEFM stress intensity factor.

If non-propagating cracks emanate from the tip of a notch weakening a real component,  $F$  is always larger than unity (Tada et al., 2000). This makes it evident that non-propagating cracks are always confined within the structural volume, even when they reach their maximum length.

All the above arguments seem to strongly support the idea that the fatigue process zone has a size which is directly related to the material characteristic length,  $L$ . The question now is "What is the material cracking behaviour within the fatigue process zone?". During the last few years, we extensively investigated crack paths within the structural volume in the high cycle fatigue regime. In particular, we considered specimens of steel weakened by different geometrical features and subjected to both uniaxial and biaxial fatigue loading (Susmel and Taylor, 2004).

Our understanding of the phenomenon is that initiation and initial growth of micro/meso-cracks are always mixed-mode governed and this process can be considered to be similar to the classical Stage 1 taking place in plain specimens (Miller, 1993). In particular, independently of stress concentration feature and degree of multiaxiality of the stress field, crack initiation is mixed-mode dominated and the length of the Stage 1-like crack is equal to about  $L/2$ . To be precise, the transition from a Stage 1-like to a Stage 2-like process occurs at a distance from the notch tip depending on the material characteristic length,  $L$ . When the crack length is larger than about  $L/2$ , cracks tend to orient themselves in order to experience the maximum Mode I loading (Stage 2-like process). Therefore, if crack initiation is assumed to be the most important stage in determining fatigue limits, it is logical to believe that the critical plane approach is the soundest method to model the physical reality.

## 2.1 The Theory of Critical Distances (TCD) and the Modified Wöhler Curve Method (MWCM)

In the recent past, Taylor has proposed a new reinterpretation of the TCD to predict uniaxial fatigue limits of components weakened by any kind of stress concentration feature (Taylor, 1999). This approach postulates that the reference stress to be used to assess notched components can be calculated in different ways. In particular, it can be determined at a certain distance from the apex of the stress concentrator (Point Method, PM), it can be averaged along a line (Line Method, LM), or, finally it can be averaged over an area (Area Method, AM). The TCD was seen to be capable of predictions falling within an error interval of about 20% (Susmel and Taylor, 2003). This method is essentially empirical, but Taylor has proposed that the LM may be related to the conditions for propagation of a notch-root crack of length  $2L$ . Unfortunately, this would only justify the use of the method for sharp notches, giving no explanation as to the reason why the TCD is also successful in predicting fatigue limits in the presence of blunt notches.

In order to formalize the TCD in terms of the PM, consider a notched specimen subjected to a remote uniaxial fatigue loading. The reference stress to be compared to the plain fatigue limit,  $\Delta\sigma_{-1}$ , can be found in different ways, as follows. For the PM the stress can be calculated at a point positioned along the notch bisector at a distance from the notch tip equal to  $L/2$  that is expressed mathematically as:

$$\sigma_{PM} = \sigma(\theta = 0, r = L/2). \quad (3)$$

For the LM the reference stress can alternatively be averaged along a line of length  $2L$  that is summarized by the following formula:

$$\sigma_{LM} = \frac{1}{2L} \int_0^{2L} \sigma(\theta = 0, r) dr. \quad (4)$$

where  $L$  is given by Eq. 1 and  $\sigma$  (Cauchy's tensor) is given by Eq. 8 or 9. It is important to highlight here that, to properly apply the TCD,  $L$  must always be determined for the correct load ratio,  $R$  (Susmel and Taylor, 2003). According to the PM, the point at which the reference stress must be calculated exactly corresponds to the centre of the structural volume.

The MWCM takes as its starting point the assumption that crack initiation is Mode II dominated, and it holds true independently of both stress concentration feature and degree of multiaxiality of the stress field damaging the fatigue process zone. The MWCM formalised to assess components in the high-cycle fatigue regime is written:

$$\tau_a + m_1 \frac{\sigma_{n,max}}{\tau_a} - \lambda = 0 \quad (5)$$

In the above equation,  $\tau_a$  is the shear stress amplitude relative to the material plane experiencing the maximum shear stress amplitude (critical plane),  $\sigma_{n,max}$  is the maximum stress perpendicular to this plane and, finally,  $\lambda$  and  $m_1$  are material constants that can be obtained from two fatigue limits generated under different loading conditions. For instance, if the fatigue limits  $\sigma_{-1}$  and  $\sigma_0$  generated under fully-reversed ( $R=-1$ ) and under repeated ( $R=0$ ) uniaxial load, respectively, are considered, the two relevant constants of the criterion turn out to be:

$$m_1 = \frac{\sigma_{-1} - \sigma_0}{2}, \quad (6)$$

$$\lambda = \sigma_{-1} - \frac{\sigma_0}{2}. \quad (7)$$

It is interesting to observe that, even though the MWCM can successfully be calibrated using two experimental uniaxial fatigue limits generated under different load ratios, when one of these two fatigue limits is estimated using a proper methodology, the MWCM accuracy becomes sensitive to the detrimental effect of non-zero mean stresses on the assessed material. In other words, it is well-known that fatigue limits under different load ratios can be estimated by using an experimental fatigue limit generated under a reference load ratio and the material static properties, but, unfortunately, the accuracy of well-known methods such as those proposed by Smith-Watson-Topper (Smith et al., 1970) or Goodman (Goodman, 1919) depends on the material fatigue behaviour under superimposed static stresses (Susmel et al., 2004).

Reliability and accuracy of the MWCM were initially checked by considering smooth specimens both in the high-cycle (Susmel and Taylor, 2003) and in the medium-cycle fatigue regime (Susmel and Petrone, 2003), showing that this method was capable of successfully accounting for the presence of both non-zero out of phase angles and non-zero mean stresses (Susmel and Taylor, 2004). Subsequently, the MWCM was applied in conjunction with the TCD to predict high-cycle fatigue strength of notched components under both uniaxial and multiaxial fatigue loading (Susmel and Taylor, 2003).

In particular, according to the arguments summarized in the previous section, it is possible to say that fatigue limits have to be estimated by considering a stress state which is representative of the entire stress field damaging the fatigue process zone. In more detail, using the PM argument, it is possible to assume that the linear-elastic stress state calculated at the centre of the structural volume supplies all of the engineering information needed to perform an accurate high-cycle fatigue assessment (Susmel and Taylor, 2003). Moreover, in fatigue limit conditions, and independently of the stress concentration feature, the crack initiation phenomenon can be assumed to be governed by a Stage 1-like process. According to this, fatigue damage reaches its maximum value on the plane experiencing the maximum shear stress amplitude, and its amount depends on both  $\tau_a$  and  $\sigma_{n,max}$  when calculated at the center of the structural volume.

## 2.2 The procedure to apply the MWCM in terms of the TCD to fretting fatigue situations

A fretted component subjected to a system of external contact forces ( $P$  and  $Q$ ) and also experiencing a bulk fatigue stress ( $\sigma_B$ ) gives rise to a subsurface multiaxial stress field within the contact region (Fig. 2). Further, as also happens to components containing geometrical discontinuities, the fretting regime is characterized by the presence of stress concentration phenomena at the contact surface which rapidly decay. This suggests that a threshold condition for crack initiation might be predicted by using methodologies similar to those employed to assess notched components. According to this idea, we seek to use the MWCM re-interpreted in terms of TCD to address the fretting fatigue problem.

In order to apply the procedure proposed in the present paper, it is initially necessary to determine the radius of the structural volume (Fig. 2). It must always be calculated using fatigue properties (that is,  $\Delta\sigma_{-1}$  and  $\Delta K_{th}$ ) determined under a load ratio,  $R$ , equal to -1 (Susmel and Taylor, 2003). In fact, as said above, the reference configuration is the one given by a through-cracked plate under fully-reversed uniaxial fatigue loading (Fig. 1a) and the presence of nonzero mean stresses as well as of non-zero out-of-phase angles is directly accounted for by Eq. 5.

It is important to remember here that in real joints some localized plasticity may be induced by the stress concentration phenomenon present at the contact interface. For this reason, a rigorous analysis to determine the stress field in the vicinity of the contact region should consider an appropriate constitutive model capable of accounting for the stress redistribution under the stress raiser. Unfortunately, these kinds of analyses are complex and time-consuming, so that, too often, they are not compatible with the industrial needs. One of the most important features of the TCD is that stress concentration phenomena in fatigue can be assessed just by carrying out linear-elastic analysis, reducing time and costs of the design process. Therefore, and taking advantage from this peculiarity of the TCD, the use of the proposed method is based on linear-elastic solutions.

When the stress tensor is entirely defined during the load cycle at the centre of the structural volume ( $y/a = L/2$  in Fig. 2), by using the appropriate algorithms (Papadopoulos, 1998, Weber et al., 1999) it is relatively simple to determine the critical plane orientation as well as the shear stress amplitude and the maximum normal stress relative to such a plane (unfortunately, dealing with complex periodic load histories, this calculation is rather time-consuming). Finally, if the condition expressed by Eq. 5 is assured, then the studied component is predicted to be in the fatigue limit condition. Figure 2 depicts a schematic view of the application of the proposed methodology to a cylinder-on-flat contact configuration under fretting conditions.

To be precise, our method takes as its starting point the idea that high-cycle fatigue damage in metals depends on both stress gradients and degree of multiaxiality of the stress field in the vicinity of crack initiation sites. Our understanding of the phenomenon is that this fact holds always true independently of the causes these two phenomena are originated from: the MWCM accounts for the multiaxiality of the stress field, whereas the TCD allows the stress gradient effect to be taken into account.

To conclude this section it is worth noting that, in general, analytical approaches are not adequate to determine the stress state at the center of the structural volume for real mechanical assemblies. For this reason, engineers engaged in

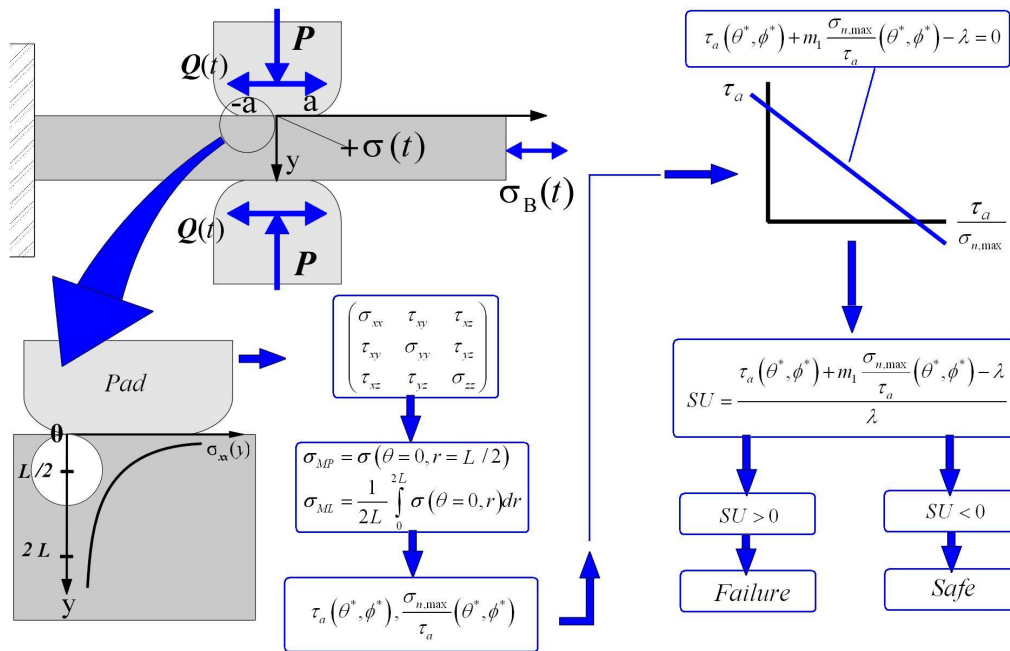


Figure 2. The procedure to apply the MWCM in terms of the TCD for fretting fatigue.

practical problems prefer to determine such stress states by post-processing FE results: the proposed methodology is suitable for being used in conjunction with linear-elastic FE results, with the advantage that parameters such as nominal stress, equivalent stress intensity, etc. do not have to be defined.

### 2.3 Available experimental data for cylindrical contacts

In the next section the proposed procedure will be validated by using experimental data for a cylinder-on-plane contact configuration (Fig 3). These experiments have been reported and discussed in detail elsewhere (Araújo et al., 2004), hence, only the basic pieces of information necessary to carry out the analysis are briefly reported below. In particular, a constant normal load,  $P$ , was applied to the fretting pads and held constant. A sinusoidal bulk load  $B(t)$  applied to "the dog bone" tensile specimen induced (i) a bulk fatigue stress,  $\sigma_B(t) = \sigma_{Bmax} \sin(\omega t)$ , and (ii) a in-phase shear load,  $Q(t) = Q_{max} \sin(\omega t)$ , where  $\sigma_{Bmax}$  and  $Q_{max}$  were the amplitudes of bulk stress and shear load, respectively,  $\omega$  was the load frequency and  $t$  was the time. Tests were designed to run in a partial slip regime, i.e.  $Q < fP$ , where the friction coefficient for the slip zones,  $f$ , was equal to 0.75. Four series of tests were considered. Within each series an average of eight tests using different pad radii varying from 12.5 to 150mm were performed. Although the pad radius changed, the surface stress field was the same for all tests in a series (but the rate of stress decay varied). This provoked a size effect in the presence of larger contact widths (or pad radii) causing fatigue failures, whereas for the smallest contacts the tests ran up to  $10^7$  cycles (here considered as infinite life) before being interrupted. The range defined by the largest contact size causing no failure and by the smallest one resulting in fatigue failures was termed critical contact size range,  $a_{crit}$ .

Table 1 reports the relevant load parameters and  $a_{crit}$  for each data set. Pads and specimens were made of an Al4%Cu alloy (Young's modulus,  $E = 74GPa$ , yield stress  $\sigma_y = 465MPa$  and ultimate tensile strength,  $\sigma_{UTS} = 500MPa$ ). Finally, it is important to highlight that in the broken specimens cracks initiated within the slip zone, at or close to the trailing edge of the contact.

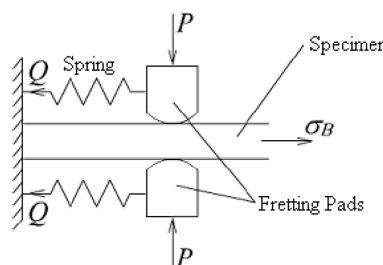


Figure 3. Cylinder on plane contact configuration.

Table 1. Experimental parameters and critical contact size range.

Series	$\sigma_{B,max}(MPa)$	$p_0(MPa)$	$Q/P$	$a_{crit}(mm)$
1	92,7	157	0,45	0,28 - 0,38
2	92,7	143	0,24	0,54 - 0,75
3	92,7	143	0,45	0,18 - 0,27
4	77,2	143	0,45	0,36 - 0,54
5	61,8	120	0,45	0,57 - 0,71

Due to the geometry of the tested configuration, the stress field in the fatigue process zone could be directly evaluated by using analytical solutions given in closed form. In particular, the direct and shear tractions could easily be defined according to the solutions proposed by Hertz (Hertz, 1882) and Mindlin (Mindlin, 1949), respectively. These could subsequently be used with Muskhelishvili's potentials (Muskhelishvili, 1953) to determine the stress components associated with the normal and the shear load. By superposing these different contributions, it was possible to directly evaluate the resulting stress tensor. In particular, at the instants of maximum and minimum bulk/shear loads it turned out to be:

$$\frac{\sigma(x, y, t)}{p_0} = \frac{\sigma^n\left(\frac{x}{a}, \frac{y}{a}\right)}{p_0} \pm f \frac{\sigma^t\left(\frac{x}{a}, \frac{y}{a}\right)}{p_0} \mp f \frac{c}{a} \frac{\sigma^t\left(\frac{x-e}{c}, \frac{y}{c}\right)}{p_0} + \frac{\sigma_B(t)}{p_0}, \quad (8)$$

being the combination of signs + and - for the maximum load step. On the contrary, during loading or unloading, the appropriate analytical solution resulted in the following form:

$$\begin{aligned} \frac{\sigma(x, y, t)}{p_0} = & \frac{\sigma^n\left(\frac{x}{a}, \frac{y}{a}\right)}{p_0} \pm f \frac{\sigma^t\left(\frac{x}{a}, \frac{y}{a}\right)}{p_0} \mp 2f \frac{d(t)}{a} \frac{\sigma^t\left(\frac{x-e'(t)}{d(t)}, \frac{y}{d(t)}\right)}{p_0} + \\ & \pm f \frac{c}{a} \frac{\sigma^t\left(\frac{x-e}{c}, \frac{y}{c}\right)}{p_0} + \frac{\sigma_B(t)}{p_0}, \end{aligned} \quad (9)$$

For unloading conditions the correct sequence of signs to be considered in Eq. (9) is: -, + and -. In the above equation,  $p_0$  is the peak pressure,  $c$  and  $e$  are the stick zone half width and its offset from the center of the contact at the instant of maximum or minimum shear load. At any other time instant  $d$  and  $e'$  correspond to the stick zone half width and its offset from the center of the contact. The superscripts  $n$  and  $t$  stand for the stress components due to the normal and the tangential load, respectively. Finally,  $\sigma_B(t)$  is the stress tensor associated with the bulk fatigue load, hence  $\sigma_{xx}$  is its unique stress component different from zero. Plane strain conditions are assumed. Explicit expressions to compute  $c$ ,  $e$ ,  $d$ ,  $e'$ ,  $\sigma^n$  and  $\sigma^t$  are given in a convenient form by Hills and Nowell (Hills and Nowell, 1994).

#### 2.4 MWCM accuracy in predicting high-cycle fatigue strength under fretting fatigue

This section summarizes the results obtained when applying the MWCM to estimate the high-cycle fatigue strength of the experimental configurations considered in this work and briefly discussed above. In order to evaluate the accuracy of the proposed methodology, the following error index (as defined by Papadopoulos (Papadopoulos, 1995)) was adopted:

$$SU = \frac{\tau_a + m_1 \frac{\sigma_{n,max}}{\tau_a} - \lambda}{\lambda} \quad (10)$$

A negative value of the above error index indicates that fatigue failure should not occur up to a number of cycles to failure theoretically equal to infinity. On the contrary, when  $SU > 0$ , the component is not in the fatigue limit condition, but, fatigue lifetime cannot be estimated (Fig. 4). It is interesting to observe also that, from an engineering point of view, a negative value of the  $SU$  index is an indication of the fact that the component dimensions could be reduced down to the limiting condition given by  $SU = 0$ .

As briefly explained above, the first step in applying the proposed procedure is to define the material characteristic length,  $L$ . Unfortunately, this experimental information was not directly available in Refs (Araújo and Nowell, 2004), for this reason it was taken from another source. In particular, Atzori et al. reported in Ref. (Susmel et al., 2005) a value for  $L$  equal to  $0.1mm$  for an Al 4%Cu alloy having the same high-cycle fatigue strength ( $\Delta\sigma_{-1} = 248MPa$ ) as the one tested by Nowell under fretting (Araújo and Nowell, 2004). According to this value the radius of the structural volume,  $L/2$ , was assumed to be equal to  $0.05mm$  (Susmel et al., 2005). At this depth and at the trailing edge of the contact zone (hot spot), i.e.  $x/a = -1$ , the cyclic stress tensor was then analytically calculated at twelve different load steps by using

Eqs (6) and (7) that gives the stress tensor for the point method,  $\sigma_{PM}$ . For the LM the cyclic stress tensor was calculated at twelve different load steps for a given number of points equally spaced over a line positioned between the points  $(-1; 0)$  and  $(-1; 2L/a)$ . After that, these stress tensors were numerically averaged by using Eq. 4 that yielded the stress tensor for the line method,  $\sigma_{LM}$ . Finally, to predict high-cycle fatigue strength under fretting, the  $SU$  index, Eq. 10, needed to be computed from these average tensors. To compute  $SU$  one needs to consider two fatigue parameters generated under different loading conditions, such as the fatigue limits under fully-reversed bending and torsion, respectively, or two uniaxial fatigue limits generated under two different load ratios,  $R$ . Susmel (Susmel *et al.*, 2005) reported two uniaxial high-cycle fatigue strengths, determined at  $10^7$  cycles to failure, for a material similar to the one considered in the present study and having  $L = 0.1mm$  ( $R = -1$ ):  $\Delta\sigma_{-1} = 248MPa$  ( $R = -1$ ) and  $\Delta\sigma_0 = 172MPa$  ( $R = 0$ ). These reference strengths were then used to calculate constants  $m_1$  and  $\lambda$  in Eqs 6 and 7, resulting in the following values:  $m_1 = 19MPa$  and  $\lambda = 81MPa$ .

Because the above relevant high-cycle fatigue strengths were extrapolated at  $10^7$  cycles to failure, the experimental results were subdivided into two different categories: for  $N_f < 10^7$  cycles to failure, the specimens were considered as broken in the medium-cycle fatigue regime, whereas, for  $N_f \geq 10^7$  cycles to failure, tests were classified as run outs. It is interesting to highlight that, as reported in Ref (Araújo *et al.*, 2004), a direct inspection of the run out specimens ( $N_f \geq 10^7$  cycles to failure) did not reveal the presence of cracks either within the fretted zones or elsewhere within the contact region.

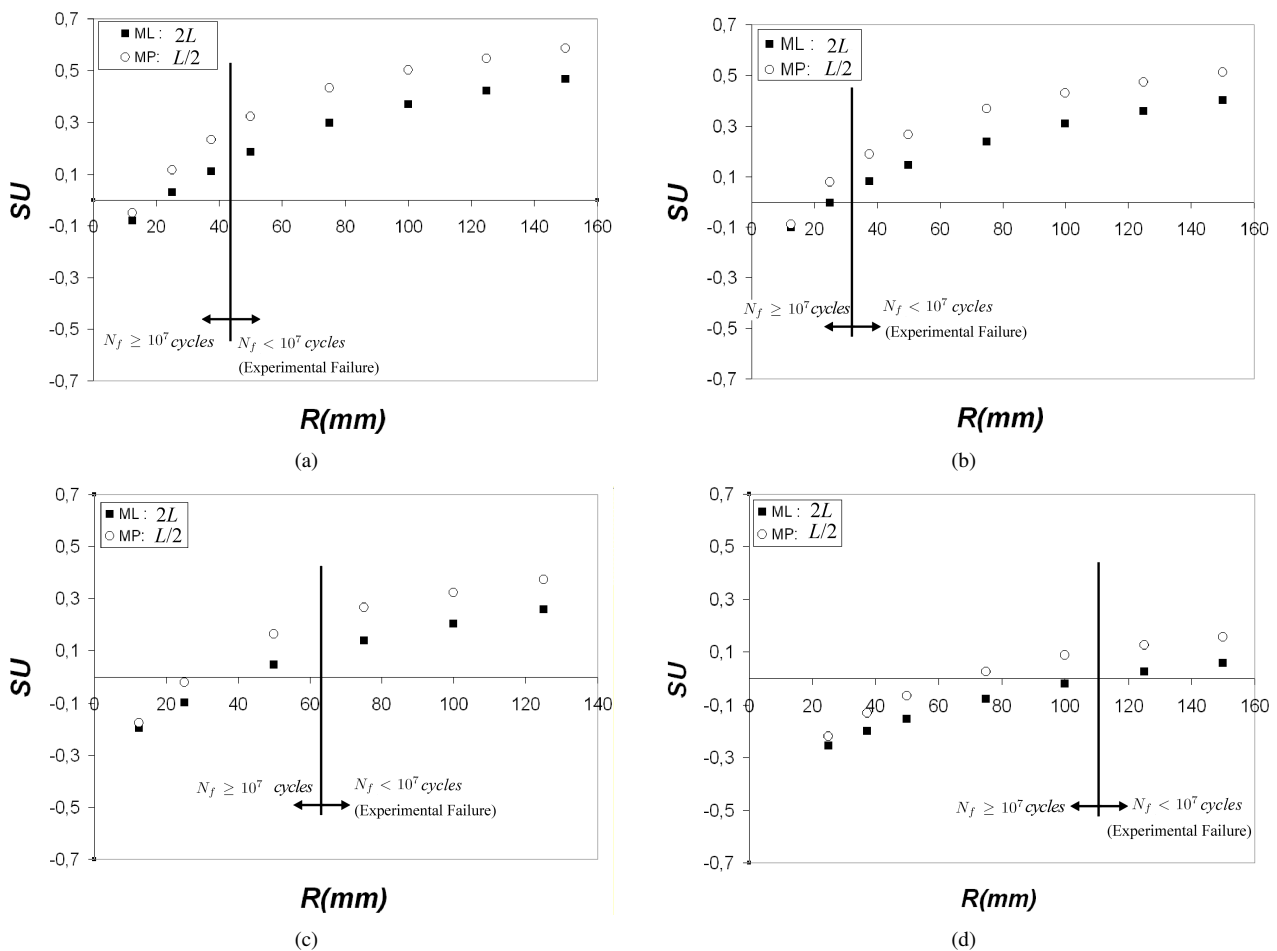


Figure 4. Error Index given by MWCM for the experimental series 1 (a), 3 (b), 4 (c) and 5 (d).

Figure 4 depicts  $SU$  compute by the PM and LM against the pad radius,  $R$ , for all tests within each experimental data series. It also shows the boundary between the tests that run out and those where failure occurred. It can be noticed that the error index always indicates failure when it takes place, however in some cases the test reached infinity life and the  $SU$  provided by PM and LM were positive indicating failure for unbroken specimens. This indicates that the two methods are conservative in the evaluation of the fatigue strength. It is also noticed in Fig 4 that the  $SU$  provided by LM were smaller than those by the PM, which indicates that the LM is less conservative than the PM, especially for larger pad radius where the stress gradient is milder, being this behavior noticed for all series. For example, in Fig. 4d ( $R = 75mm$  and  $R = 100mm$ ) and in Fig 4b ( $R = 25mm$ ), the tests experienced infinity life and the PM indicated failure while the LM indicated, correctly, safe life.

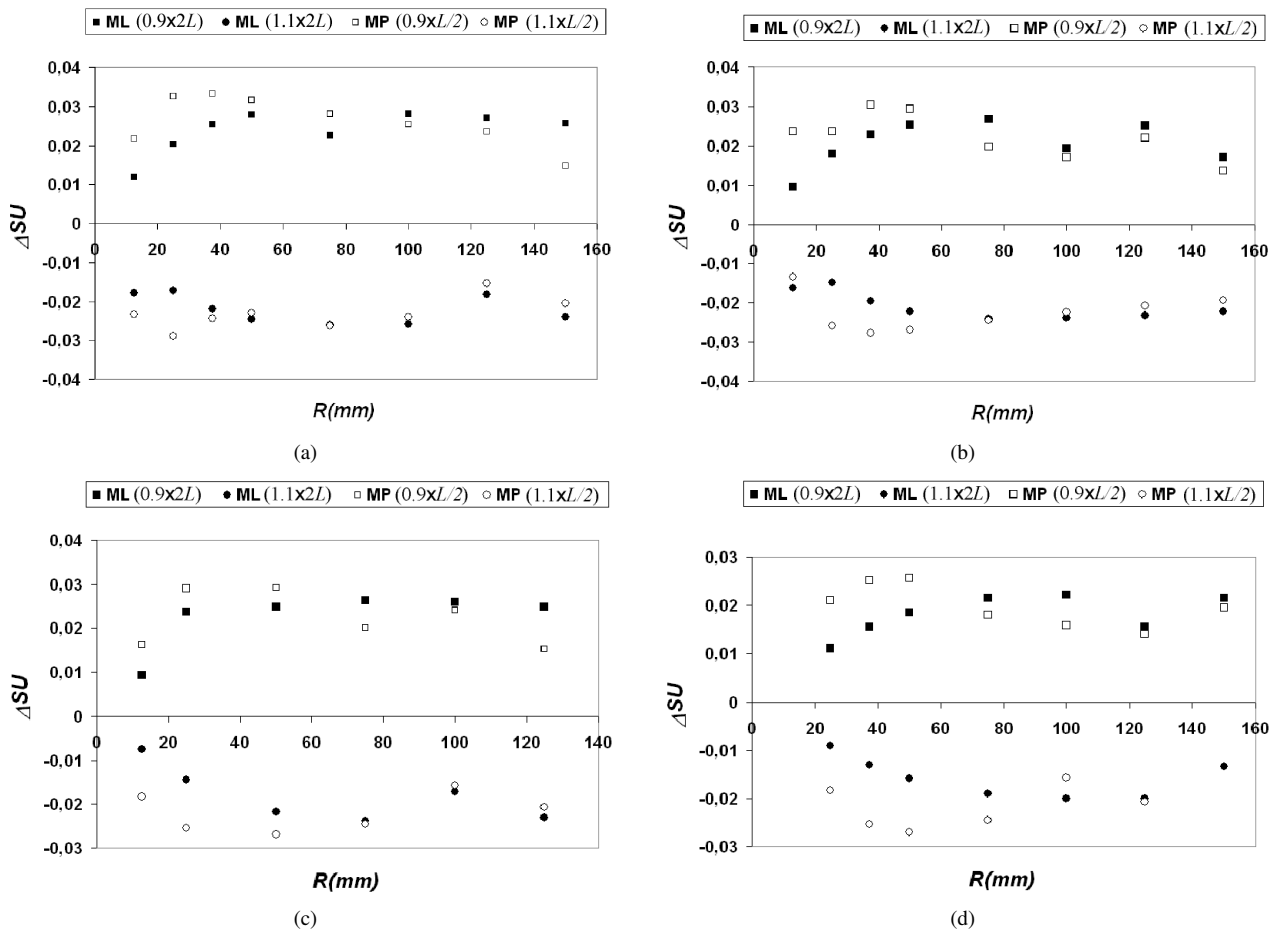


Figure 5. Variation of the Error Index  $SU$  for the PM and LM according to a variation of 10% in the parameter  $L$  (Series 1 (a), 3 (b), 4 (c) and 5 (d)).

Being the parameter  $L$  a material property that is subjected to experimental uncertainties in its determination, it seems important to understand how its variation affects the results provided by the proposed methodology. In order to take into account this effect, it was supposed a variation of  $L$  between +10% and -10% from the reported nominal value  $L = 0.1\text{mm}$ . Figure 5 shows the error index variation with respect to the nominal position ( $\Delta SU$ ) for each pad radius considering experimental series 1, 3, 4 and 5 according to the proposed analysis. It seems clear from these graphs that the LM is less sensitive to the variation of  $L$  than the PM for more severe stress gradient conditions, in other words, for smaller pad radii. A reduction in  $L$  essentially means that the evaluation of the average stress is conducted closer to the contact surface leading therefore to more severe solicitation which, in turn, will provide  $\Delta SU > 0$ . The opposite behavior takes place when the  $L$  increases. This variation has a decisive influence on the evaluation of the fatigue strength for tests that had small error index ( $|SU| < 3\%$ ) and can be responsible for an evaluation of failure or safe life.

### 3. DISCUSSION AND CONCLUSION

This paper is a continuity of previous work by Araújo et al. (2006), and its aim was to propose a methodology to estimate the fatigue strength limit under fretting conditions. Such methodology was validated for experimental results taken from the literature involving the contact between cylindrical pads and a flat tensile "dog bone" specimen. The proposed methodology is founded on the use of the Theory of Critical Distance associated with the multiaxial fatigue model proposed by Susmel & Lazzarin (Modified Wöhler Curve Method). The results provided by the Line Method and the Point Method were compared showing that the Line Method has correctly evaluated the fatigue strength for 26 of the 29 experimental tests considered in this work, against 23 of 29 for the Point Method. Both methods were also compared concerning their sensibility to an increase or decrease of 10% on the value of the material parameter, which is used to determine the critical distance. The results have shown that the Line Method is less sensitive than the Point Method to this parameter for situations of high stress gradients (smaller contacts).

#### 4. REFERENCES

- Akiniwa, Y., Tanaka, K., Kimura, H., 2001, "Microstructural effects on crack closure and propagation thresholds of small fatigue cracks". *Fatigue Fract. Engng. Mater. Struct.* 24, 817-831.
- Araújo, J.A., Susmel, L., Taylor, D., Ferro, J.C.T, Mamiya, E.N., 2006, "On the use of the Theory of Critical Distances and the Modified Wöhler Curve Method to estimate fretting fatigue strength of cylindrical contacts". *International Journal of Fatigue* 29 (2007) 95-107
- Araújo, J.A., Nowell, D. and Vivacqua, R. C., 2004, "The use of multiaxial fatigue models to predict fretting fatigue life of components subjected to different contact stress fields". *Fatigue Fract Engng Mater Struct* 27, 967-978.
- Araújo, J.A., Nowell, D., 1999, "Analysis of pad size effects in fretting fatigue using short crack arrest methodologies". *Int. J. Fatigue* 21 9, 947-956.
- Dowling, N., 2004, "Mean Stress Effects in Stress-Life and Strain-Life Fatigue", 2nd SAE Brasil International Conference on Fatigue, São Paulo, 22-23th June 2004.
- Goodman, J., 1919, "Mechanics Applied to Engineering", Longmans, Green and Co., London, 631-636.
- Hertz, H., 1882, "Über die Berührung fester elastischer Körper", *Jnl. Reine und angewandte Mathematik* 92, 156- 171.
- Hills, D. A. and Nowell, D., 1994, "Mechanics of fretting fatigue". Kluwer Academic publishers, Dordrecht, 1994.
- Miller, K. J., 1993, "The two thresholds of fatigue behaviour". *Fatigue Fract. Engng. Mater. Struct.* 16, 931-939.
- Mindlin, R. D., 1949, "Compliance of elastic bodies in contact". *Jnl. App. Mech.* 16, 259-268.
- Muskhelishvili, N. I., 1953, "Some Basic Problems of Mathematical Theory of Elasticity". Noordhoff, Gröningen.
- Nowell, D., 1988, "An analysis of fretting fatigue", D. Phil. thesis, Oxford University.
- Papadopoulos, I.V., 1998, "Critical Plane Approaches in High-Cycle Fatigue: on the Definition of the Amplitude and Mean Value of the Shear Stress Acting on the Critical Plane". *Fatigue Fract. Engng. Mater. Struct.* 21, 269-285.
- Papadopoulos, I. V., 1995, "A High-Cycle Fatigue Criterion applied in Biaxial and Triaxial Out-of-Phase stress conditions". *Fatigue Fract. Engng Mater. Struct.* 18, 79-91.
- Smith, K.N., Watson, P., and Topper, T.H., 1970, "A Stress-Strain Function for the Fatigue of Metals", *J. Mater.* 5 4, 767-778.
- Susmel, L., Atzori, B., Meneguetti, G., 2005, "Material fatigue properties for assessing mechanical components weakened by notches and defects". *Fatigue Fract. Engng. Mater. Struct* 28, 1-15.
- Susmel, L., Taylor, D., 2004, "Non-propagating cracks under in-phase mode I and II loadings". In: F. Nilsson (Ed.), *Proc. of 15th European Conference of Fracture, Stockholm (Sweden), August 11-13, 2004.*
- Susmel, L., Taylor, D., 2003, "Two methods for predicting the multiaxial fatigue limits of sharp notches". *Fatigue Fract. Engng. Mater. Struct.* 26, 821-833.
- Susmel, L., Petrone, N., 2003, "Multiaxial fatigue life estimations for 6082-T6 cylindrical specimens under in-phase and out-of-phase biaxial loadings". In: A. Carpinteri, M. de Freitas and A. Spagnoli (Ed.), *Biaxial and Multiaxial fatigue and Fracture*, Elsevier Science Ltd. and ESIS, Oxford, 83-104.
- Tada, H., Paris, C. P.; Irwin, R. G., 2000, "The Stress Analysis of Cracks  $\checkmark$  Handbook". Professional Engineering Publishing, Bury St. Edmunds, UK (Third Edition).
- Taylor, D., 1999, "Geometrical effects in fatigue: a unifying theoretical model". *Int. J. Fatigue* 21, 413-420.
- Vallelano, C., Dominguez, J., Navarro, A., 2004, "Predicting the fretting fatigue limit for spherical contact". *Engineering Failure Analysis* 11, 727-736.
- Weber, B., Kenneugne, B., Clement, J. C., Robert, J. L., 1999, "Improvements of multiaxial fatigue criteria computation for a strong reduction of calculation duration". *Computational Materials Science* 15, 381-399.

#### 5. Responsibility notice

The author(s) is (are) the only responsible for the printed material included in this paper